

## TMEFF2 Deregulation Contributes to Gastric Carcinogenesis and Indicates Poor Survival Outcome

Tiantian Sun<sup>1</sup>, Wan Du<sup>1</sup>, Hua Xiong<sup>1</sup>, Yanan Yu<sup>1</sup>, Yurong Weng<sup>1</sup>, Linlin Ren<sup>1</sup>, Huijun Zhao<sup>1</sup>, Yingchao Wang<sup>1</sup>, Yingxuan Chen<sup>1</sup>, Jie Xu<sup>1</sup>, Yongbing Xiang<sup>1</sup>, Wenxin Qin<sup>1</sup>, Weibiao Cao<sup>2</sup>, Weiping Zou<sup>3</sup>, Haoyan Chen<sup>1</sup>, Jie Hong<sup>1,2</sup>, and Jing-Yuan Fang<sup>1</sup>

### Abstract

**Purpose:** The role and clinical implication of the transmembrane protein with EGF and two follistatin motifs 2 (TMEFF2) in gastric cancer is poorly understood.

**Experimental Design:** Gene expression profile analyses were performed and Gene Set Enrichment Analysis (GSEA) was used to explore its gene signatures. AGS and MKN45 cells were transfected with TMEFF2 or control plasmids and analyzed for gene expression patterns, proliferation, and apoptosis. TMEFF2 expression was knocked down with shRNAs, and the effects on genome stability were assessed. Interactions between TMEFF2 and SHP-1 were determined by mass spectrometry and immunoprecipitation assays.

**Results:** Integrated analysis revealed that TMEFF2 expression was significantly decreased in gastric cancer cases and its expression was negatively correlated with the poor pathologic stage, large tumor size, and poor prognosis. GSEA in The Cancer Genome Atlas (TCGA) and Jilin datasets revealed that cell proliferation, apoptosis, and DNA damage-related genes were enriched in TMEFF2 lower expression patients. Gain of TMEFF2 function decreased cell proliferation by increasing of apoptosis and blocking of cell cycle in gastric cancer cells. The protein tyrosine phosphatase SHP-1 was identified as a binding partner of TMEFF2 and mediator of TMEFF2 function. TMEFF2 expression positively correlated with SHP-1, and a favorable prognosis was more likely in patients with gastric cancer with higher levels of both TMEFF2 and SHP-1.

**Conclusion:** TMEFF2 acts as a tumor suppressor in gastric cancer through direct interaction with SHP-1 and can be a potential biomarker of carcinogenesis. *Clin Cancer Res*; 20(17); 4689–704. ©2014 AACR.

### Introduction

Gastric cancer is the fourth most highly diagnosed type of cancer and the second most common cause of cancer-

related death worldwide (1). Most patients are only diagnosed at an advantaged stage due to a lack of early specific symptoms. Patients with advanced gastric cancer have a poor prognosis and eventually die after surgery as a result of cancer recurrence and metastasis (2, 3). Pathologic classification is currently the most important tool used to assess prognosis and inform the treatment of gastric cancer. The roles of genetic changes, epigenetic alterations, and signaling pathways involved in cancer have recently been studied intensively (4–6). The use of gene expression data to predict tumorigenesis holds promise in gastric cancer diagnosis. However, many putative pro-cancer genetic changes occur in histologically normal tissue well before the onset of dysplasia. Therefore, more research is needed to discover and develop more effective biomarkers for gastric cancer diagnosis.

The transmembrane protein with EGF and two follistatin motifs 2 (TMEFF2) gene encodes a putative transmembrane protein containing 2 follistatin-like domains and an EGF-like domain (7). It is expressed in the embryo and selectively in the adult brain and prostate (8–10). As a recently discovered gene, TMEFF2 is epigenetically silenced in a number of tumor types (11–13). In contrast, the shed form of TMEFF2 is able to induce ERK1/2 phosphorylation and contribute to cell proliferation in prostate cancer cells in

<sup>1</sup>State Key Laboratory for Oncogenes and Related Genes, Key Laboratory of Gastroenterology and Hepatology, Ministry of Health, Division of Gastroenterology and Hepatology, Renji Hospital, School of Medicine, Shanghai Jiao Tong University, Shanghai Cancer Institute, Shanghai Institute of Digestive Disease, Shanghai, China. <sup>2</sup>Department of Pathology and Medicine, The Warren Alpert Medical School of Brown University and Rhode Island Hospital, Providence, Rhode Island. <sup>3</sup>Department of Surgery, University of Michigan, Ann Arbor, Michigan.

**Note:** Supplementary data for this article are available at Clinical Cancer Research Online (<http://clincancerres.aacrjournals.org/>).

T. Sun, W. Du, and H. Xiong contributed equally to this article.

Transcript Profiling: The gene expression data have been deposited in NCBI's Gene Expression Omnibus (GEO, <http://www.ncbi.nlm.nih.gov/geo/>) and are accessible through GEO Series accession number GSE49052.

**Corresponding Authors:** Jie Hong, Shanghai Jiao-Tong University School of Medicine Renji Hospital, 145 Middle Shandong Road, Shanghai 200001, China. Phone: 86-2153882450; Fax: 86-2163266027; E-mail: jiehong97@gmail.com; Haoyan Chen, chenhaoyan@gmail.com; and Jing-Yuan Fang, jingyuanfang@yahoo.com

doi: 10.1158/1078-0432.CCR-14-0315

©2014 American Association for Cancer Research.

### Translational Relevance

The mRNA expression microarray shows that two follistatin motifs 2 (TMEFF2) is decreased in gastric cancer tissues; however, its role and clinical implication in gastric cancer is poorly understood. We demonstrate for the first time that TMEFF2 may be a potential biomarker to predict gastric carcinogenesis via altering tumorigenesis gene signatures and acts as a tumor suppressor in gastric cancer through direct interaction with SHP-1. TMEFF2 expression was gradually decreased from normal gastric tissue through to precancerous lesions and then to gastric cancer, and its expression was negatively correlated with the poor pathologic stage, large tumor size, and poor prognosis. Gene Set Enrichment Analysis (GSEA) revealed that cell proliferation, apoptosis, and DNA damage-related genes were enriched in TMEFF2 lower expression patients. The protein tyrosine phosphatase SHP-1 was identified as a binding partner of TMEFF2 and mediator of TMEFF2 function. A favorable prognosis was more likely in patients with gastric cancer with higher levels of both TMEFF2 and SHP-1.

response to phorbol ester treatment (14). Therefore, the biologic function of TMEFF2 remains poorly understood because conflicting reports indicate both a positive and a negative association between TMEFF2 and human cancers.

In this study, we show that TMEFF2 expression is significantly decreased in gastric cancer tissues when compared with normal gastric tissues. Functional assays and Genome Set Enrichment Analysis (GSEA) confirmed that TMEFF2 acts as a tumor suppressor by regulating cell proliferation, apoptosis, and genomic stability. We also evaluated the biologic function and clinical application of TMEFF2 in gastric cancer and identified the protein tyrosine phosphatase (PTP) SHP-1 as the major interacting protein with TMEFF2.

### Materials and Methods

#### The three individual datasets collection

Tumor, the adjacent, and normal gastric specimens were obtained from patients with gastric cancer who underwent surgery at Shanghai Renji Hospital (Shanghai, China) from February 1995 to May 2004. The study protocol was approved by the ethics committee of Shanghai Jiao Tong University School of Medicine, Renji Hospital. Written informed consents were obtained from all participants in this study. All the research was carried out in accordance with the provisions of the Helsinki Declaration of 1975. None of these patients had received radiotherapy or chemotherapy. The percentage of tumor cellularity in the gastric cancer patient's tissue section is at least 70% via pathologic examination of histology slides in Renji patient's cohort. A written informed consent was obtained from all

patients in Jinlin dataset, which was approved by the Institutional Review Board (IRB) at the University of Georgia (Athens, GA). All samples in The Cancer Genome Atlas (TCGA) have been collected and used following strict human subjects protection guidelines, informed consent, and IRB review of protocols.

#### Bioinformatics analysis

Six gastric mucosal tissues (including 3 normal gastric mucosa and 3 tumor tissues) with written informed consent were obtained. Total RNA from each sample was isolated, and Agilent Array platform was used for microarray analysis. The RNA was isolated and analyzed by HOA v6 human one array microarray analysis in human GC cells (AGS), after transfection with TMEFF2 overexpression plasmid or control, respectively. The gene expression data have been deposited in NCBI's Gene Expression Omnibus (GEO, <http://www.ncbi.nlm.nih.gov/geo/>) and are accessible through GEO Series accession number GES49052.

Human exon arrays for gastric cancer and normal adjacent tissue were downloaded from the GEO. The datasets GSE27342 consisted of 80 paired gastric cancer and normal adjacent tissue. All samples were taken from 3 hospitals affiliated with Jilin University College of Medicine and Jilin Provincial Cancer Hospital, Changchun, China. TCGA RNA-Seq (level 3) and corresponding clinical data were downloaded from TCGA website (<https://tcga-data.nci.nih.gov/tcga/>) following approval of this project by the consortium. RNA-Seq analysis used data from 274 gastric cancers and 33 adjacent normal tissues. The mutation counts and fraction of copy number altered genome data for each TCGA gastric cancer individual were directly downloaded from the cBioPortal for Cancer Genomics (<http://cbioportal.org>). To gain further insight into the biologic pathways involved in gastric cancer pathogenesis through TMEFF2 pathway, a GSEA was performed. The gene sets showing FDR of 0.25, a well-established cutoff for the identification of biologically relevant gene, were considered enriched between classes under comparison. The GO gene sets biological process database (c5.bp.v4.0) from the Molecular Signatures Database–MsigDB (<http://www.broad.mit.edu/gsea/msigdb/index.jsp>) were used for enrichment analysis. Only gene sets represented by at least 15 genes were retained.

#### Patient specimens

Human gastric mucosal tissues (normal tissues, tissues diagnosed with IM or DYS) were collected from patients made gastroscopy inspection in Renji hospital with written informed consent. None of the patients had taken NSAIDs, H2 receptor antagonists, proton pump inhibitors, antimicrobials, or bismuth compounds in the 4 weeks before the study. The different extent of inflammation in these tissues was examined according to the updated Sydney System (International Workshop on the Histopathology of Gastritis, Houston, 1994) and is listed in Supplementary Table S1.

### Cell culture and treatment

The human gastric epithelial cell line GES-1 and gastric cancer cells (AGS, MKN45, MGC803, SGC7901, MKN28) were cultured in RPMI-1640 medium (Gibco) supplemented with 10% FBS at 37°C in an atmosphere of 5% CO<sub>2</sub>. The siRNAs (50 nmol/L) against human TMEFF2 and SHP-1 were transfected into the gastric cells using the DharmaFECT 1 siRNA transfection reagent (Thermo Scientific Dharmacon Inc.), whereas nonspecific siRNA was used as negative controls. SHP-1 siRNA, TMEFF2 siRNA, and the control siRNA were purchased from Dharmacon RNA Technology. The plasmids and mutagenesis about human TMEFF2 (GenBank accession number NM\_016192) and human SHP-1 (GenBank accession number NM\_080548) were transfected into the gastric cells using the FuGENE transfection reagent (Life Technologies), whereas nonspecific plasmid was used as negative controls.

### Cell proliferation assay, cell-cycle analysis, apoptosis detection, and TUNEL reaction

Cell proliferation was assessed by the bromodeoxyuridine (BrdUrd) incorporation assay (Roche Molecular Biochemicals). Briefly, control and treated gastric cancer cells were seeded onto the 96-well plates at an initial density of  $5 \times 10^3$  cells per well. BrdUrd labeling solution (10  $\mu$ L/well) was added to the cells at specified time points. After incubating for 2 hours, culture medium was removed and the cells were fixed. Then DNA was denatured by adding Fix-Denat (200  $\mu$ L/well) and then anti-BrdUrd-POD working solution (100  $\mu$ L/well) was added to the cells and incubated for 90 minutes. The immune complexes were detected by the subsequent substrate reaction. The reaction product was quantified by measuring the absorbance at 370 nm (reference wavelength:  $\sim$ 492 nm).

Cell cycles were examined using propidium iodide (PI) and flow cytometry. Cells were fixed in cold ethanol for 30 minutes and then incubated with propidium iodide for 30 minutes before flow cytometer analysis (BD Biosciences).

Apoptosis was also determined by flow cytometric analysis. An Annexin V FITC/PI double stain assay (Biovision Inc.) was performed following the manufacturer's protocol. Both floating and trypsinized adherent cells were collected, resuspended in 500  $\mu$ L of binding buffer containing 2.5  $\mu$ L of Annexin V FITC and 5  $\mu$ L of PI, and then incubated for 5 minutes in the dark at room temperature before flow cytometric analysis.

Apoptosis of the xenograft model was detected by terminal deoxynucleotidyl transferase-mediated dUTP nick end labeling (TUNEL) technology using the In Situ Cell Death Detection Kit (Roche Molecular Biochemicals) according to standard protocols. The negative control was incubated with label solution (without terminal transferase) instead of TUNEL reaction mixture.

### Immunohistochemical staining

The expressions of TMEFF2, SHP-1, and Ki67 were examined with primary antibodies (TMEFF2, 1:200; SHP-1, 1:400; Ki67, 1:100) using the LSAB+ kit (DakoCytomation)

according to the manufacturer's instructions. The tissue slides were examined independently by 2 investigators blinded to both the clinical and pathologic data. Protein expression was quantified using a visual grading system based on the extent of staining (percentage of positive tumor cells on a scale of 0–4: 0, none; 1, 1%–25%; 2, 26%–50%; 3, 51%–75%; 4, >75%) and the intensity of staining (graded on a scale of 0–3: 0, no staining; 1, weak staining; 2, moderate staining; 3, strong staining). For further analysis, the product of the extent and intensity grades was used to define the cutoff value for higher protein expression. Therefore, protein expression was thus classified into 2 categories: high level (grades 4–12) and low level (grades 0–3).

### Immunofluorescence

For immunofluorescence of cultured cells, the AGS cells were plated into 4-well chamber slides and cotransfected with pCDNA3.1-TMEFF2WT and pCDNA3.1-SHP-1WT plasmids. Cells were fixed with 4% formaldehyde 48 hours after transfection. Then the cells were permeabilized with 0.2% Triton X-100 and blocked in 1% BSA in PBS. Secondary antibodies (Alexa488-anti-rabbit and Alexa546-anti-mouse) were used to label TMEFF2 and SHP-1.

### RNA extraction and quantitative real-time PCR

The mRNA levels were measured using a real-time quantitative PCR system. Total RNA was extracted by TRIzol reagent (Invitrogen), and 1  $\mu$ g of total RNA was reverse transcribed using the PrimeScript<sup>®</sup> RT Reagent Kit (Perfect Real Time; Takara). The amplified transcript level of each specific gene was normalized to that of 18S. The primers were provided by Sheng Gong Company. The sequences of forward and reverse primers are shown in Supplementary Table S2.

### Western blotting

Western blot assays were performed using standard techniques as described previously (15). GAPDH antibody was used as a control for whole-cell lysates. Antibodies were purchased from Cell Signaling Technology Inc., except for GAPDH (Kangchen) and TMEFF2 (Abcam).

### LC/MS analysis and database search and protein identification

The TMEFF2-flag overexpression plasmid was introduced into AGS cells, and the TMEFF2-interacting complex was purified using anti-FLAG beads. To identify specific TMEFF2 interactors, TMEFF2 and empty vector affinity eluates were compared and the bands that were mainly represented only in the TMEFF2 coimmunoprecipitated sample were chosen. The bands were excised to perform in-gel trypsin digestion, peptide extraction, and LC/MS identification. LC/MS analysis was performed on a nano Acquity UPLC system (Waters Corporation) connected to a LTQ Orbitrap XL mass spectrometer (Thermo Scientific) equipped with an online nano-electrospray ion source (Michrom Bioresources). Peptides were resuspended with 12  $\mu$ L solvent A (5% acetonitrile, 0.1% formic acid in water). About 10  $\mu$ L peptide

solution was loaded onto the Captrap Peptide column ( $2 \times 0.5 \text{ mm}^2$ , Michrom Bioresources) at a  $20 \mu\text{L}/\text{min}$  flow rate of solvent A for 5 minutes and then was separated on a Magic C18AQ reverse-phase column ( $100 \mu\text{m id} \times 15 \text{ cm}$ , Michrom Bioresources) with a 3-step linear gradient. Starting from 5% B (90% acetonitrile, 0.1% formic acid in water) to 45% B (in other words, from 95% A to 55% A, the same below) in 100 minutes, increased to 80% B in 3 minutes, and then to 5% B in 2 minutes. The column was re-equilibrated at initial conditions for 15 minutes. The column flow rate was maintained at  $500 \text{ nL}/\text{min}$  and column temperature was maintained at  $35^\circ\text{C}$ . The electrospray voltage of  $1.8 \text{ kV}$  versus the inlet of the mass spectrometer was used.

LTQ Orbitrap XL mass spectrometer was operated in the data-dependent mode to switch automatically between MS and MS/MS acquisition. Survey full-scan MS spectra with one microscan ( $m/z$ : 300–1,800) was acquired in the Orbitrap with a mass resolution of 60,000 at  $m/z$  400, followed by MS/MS of the 8 most-intense peptide ions in the LTQ analyzer. The automatic gain control (AGC) was set to 1,000,000 ions, with maximum accumulation times of 500 ms. For MS/MS, we used an isolation window of 2  $m/z$  and the AGC of LTQ was set to 20,000 ions, with maximum accumulation time of 120 ms. Single-charge state was rejected and dynamic exclusion was used with 2 microscans in 10- and 90-second exclusion duration. For MS/MS, precursor ions were activated using 35% normalized collision energy at the default activation  $q$  of 0.25 and an activation time of 30 ms. The spectrum were recorded with Xcalibur (version 2.2.0) software.

The mass spectra were searched using the Mascot Daemon software (Version 2.3.0, Matrix Science) based on the Mascot algorithm. The database used to search was the human UniProtKB/Swiss-Prot database (Release 2012\_12\_14, with 20233 entries). To reduce false-positive identification results, a decoy database containing the reverse sequences was appended to the database. The searching parameters were set up as follows: full trypsin (KR) cleavage with 2 missed cleavage was considered. Oxidation on methionine and acetylation of the protein *N*-terminus were set as variable modifications. The peptide mass tolerance was 10 ppm and the fragment ion tolerance was 1.0 Da. Peptides with Mascot scores exceeding the 99% confidence level score were accepted as correct matches (Ions score  $\geq 28$ ).

#### Purification of TMEFF2-interacting complex, protein digestion, and peptide extraction

Anti-FLAG beads (A2220) was purchased from Sigma-Aldrich; sequencing-grade trypsin (V5113) was purchased from Promega. Cells maintained in  $10 \times 100 \text{ mm}^2$  dishes were either transfected with empty vector (16  $\mu\text{g}$ ) or  $3 \times$  FLAG-tagged TMEFF2 (16  $\mu\text{g}$ ), respectively. Forty-eight hours later, cells were lysed with lysis buffer (Beyotime, P0013C) supplemented with protease inhibitor cocktail and phosphatase inhibitor cocktail (Kangchen company, KC-440). The cell lysate derived from each group (empty vector vs.  $3 \times$  FLAG-tagged TMEFF2) was precleared by incubation with (30  $\mu\text{L}$ ) mouse IgG beads (Sigma-Aldrich,

A0910) at  $4^\circ\text{C}$  for 2 hours, then followed by incubation with anti-FLAG beads (70  $\mu\text{L}$ ) at  $4^\circ\text{C}$  for 4 hours, respectively. After immunoprecipitation, anti-FLAG beads were washed for 5 times with TBS buffer [50 mmol/L Tris-HCl (pH 7.4), 150 mmol/L NaCl] to eliminate the nonspecific binding, respectively. Immunoprecipitates were then eluted by 100  $\mu\text{g}/\text{mL}$  of  $3 \times$  FLAG peptide (Sigma-Aldrich) and concentrated to the appropriate volume, respectively, for the following SDS-PAGE separation and Coomassie Blue staining. In contrast to the control (sample pulled-down from empty vector-transfected cells), the bands only in sample pulled-down from TMEFF2-transfected cells were excised for the following in-gel trypsin digestion. The procedure of visible bands excision, in-gel trypsin digestion, and peptide extraction was performed following the previously described protocol (16).

#### Coimmunoprecipitation and GST pull-down analysis

Coimmunoprecipitation (Co-IP) was performed as described previously (17). Both the input and IP samples were analyzed by Western blotting using various antibodies at the following dilutions: TMEFF2 antibody (1:1,000; Abcam), SHP-1 antibody (1:1,000), Flag-tag antibody (1:1,000), HA-tag antibody (1:1,000; Cell Signaling Technology), and normal rabbit/mouse IgG (Upstate).

GST protein and GST/SHP-1 fusion proteins were expressed and purified according to manufacturer's instructions (GE Healthcare). For the pull-down assay, 1 to 5 mg of the GST or GST fusion proteins were mixed with 40 mL of a 50% suspension of glutathione-Sepharose 4B beads for 2 hours in binding buffer [25 mmol/L HEPES-NaOH (pH 7.5), 12.5 mmol/L  $\text{MgCl}_2$ , 10% glycerol, 5 mmol/L dithiothreitol (DTT), 0.1% NP-40, 150 mmol/L KCl, and 20 mmol/L  $\text{ZnCl}_2$ ]. Then 1 to 5 mg of purified TMEFF2 protein (Abcam) was added followed by incubation for another 2 hours. The pellets were washed extensively and were identified by Western blotting: TMEFF2 antibody and GST antibody (1:1,000; Cell Signaling Technology).

#### Plasmids and mutagenesis

The DNA fragment encoding the TMEFF2 gene (GenBank accession number NM\_016192) was amplified from human cDNA with the primers TMEFF2F 5'-GGATCCATGGACTACAAAGACCATGACGGTGATTATAAAGATCATGACATCGATTACAAGGATGACGATGACAAGATGGTGCTGTGGGAGTCCCC-3' and TMEFF2R 5'-CTCGAGATTGATTAACCTCGTGGACGCTCT-3', which introduced the cloning sites *Bam*HI and *Xho*I (underlined), respectively. The cDNA fragment obtained above was verified by sequencing and finally cloned into pCDNA3.1 between the *Bam*HI and *Xho*I sites to obtain pCDNA3.1-TMEFF2WT with Flag tag.

The TMEFF2  $\Delta$ ID DNA fragment was amplified from pCDNA3.1-TMEFF2WT with the primers  $\Delta$ ID-F 5'-GGATCCATGGACTACAAAGACCATGACGGTGATTAT AAAGATCATGACATCGATTACAAGGATGACGATGACAAGATGGTGCTGTGGGAGTCCCC-3' and  $\Delta$ ID-R 5'-CTCGAGTTAGATGCAGAGGACC, which introduced the cloning sites

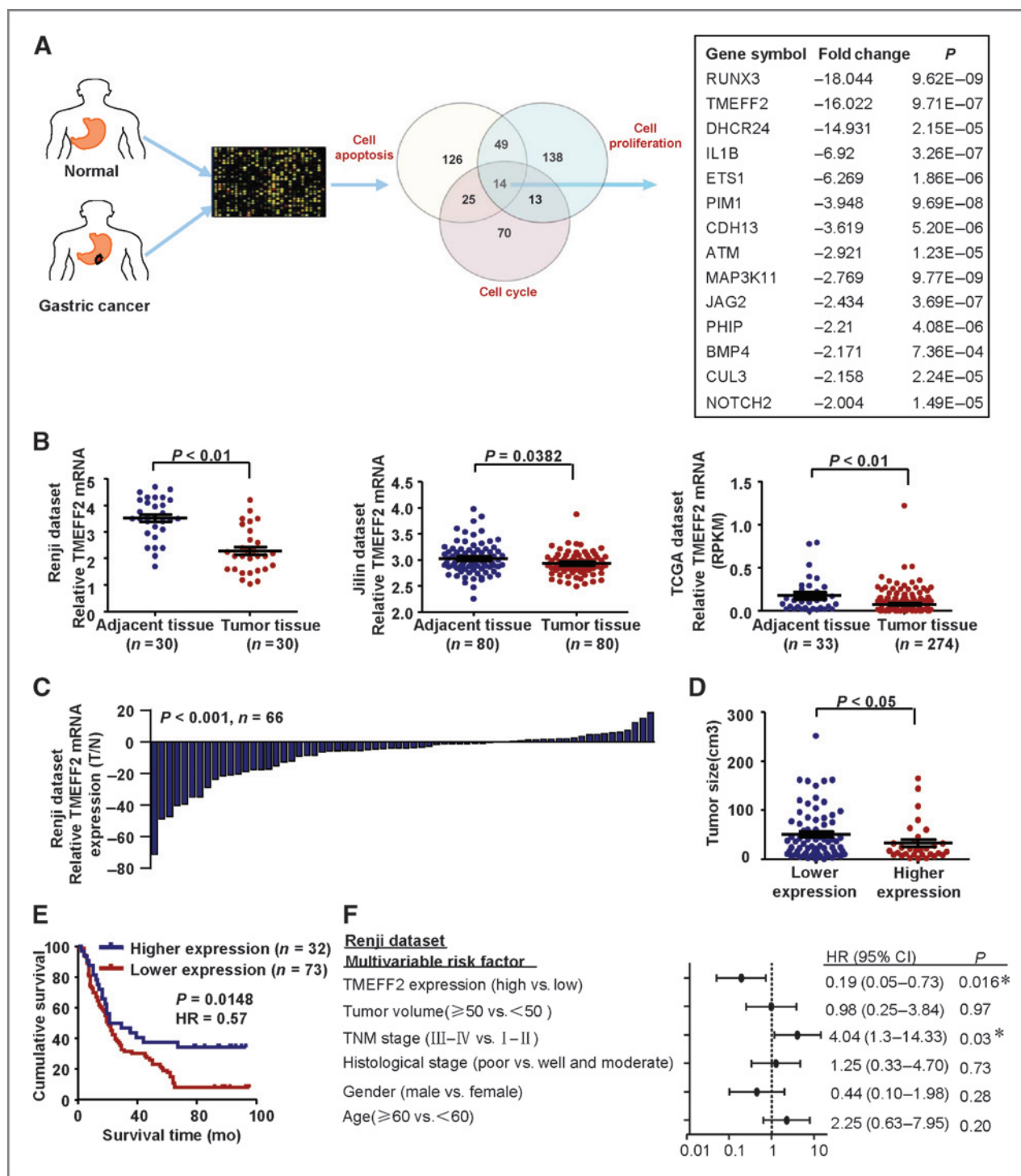
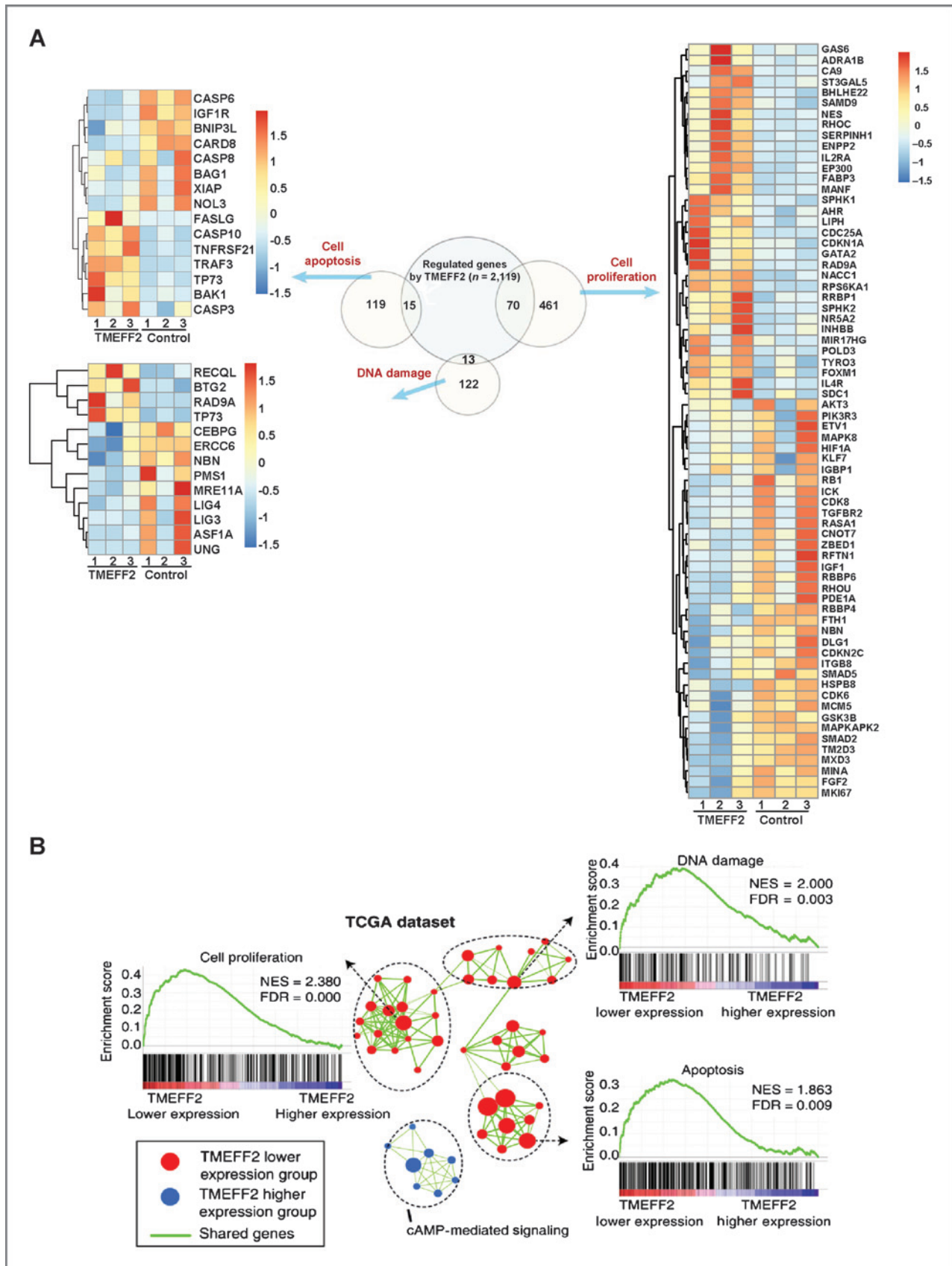


Figure 1. TMEFF2 downregulation correlates with poor survival in patients with gastric cancer. A, overview of the microarray analysis used to identify the differential gene expression between gastric cancer and normal gastric tissues. B, analysis of TMEFF2 expression in gastric cancer and their preneoplastic adjacent mucosa in 3 independent datasets: Renji dataset (nonparametric Mann-Whitney test), Jilin dataset (nonparametric Mann-Whitney test). Generalized linear model (GLM) analysis was performed for TCGA RNA-sequence data. C, analysis of TMEFF2 expression in gastric cancer and their matched adjacent mucosa in Renji dataset.  $n = 66$ , paired sample  $t$  test. D, statistical analysis on the tumor size of gastric cancer in TMEFF2 higher expression ( $n = 32$ ) and lower expression ( $n = 73$ ) groups ( $P < 0.05$ , nonparametric Mann-Whitney test). E, survival analysis showed that TMEFF2 higher expression tumors have a favorable prognosis than TMEFF2 lower expression tumors ( $P = 0.0148$ ; HR, 0.57; 95% CI, 0.37-0.90; Mantel-Cox test). F, multivariable analysis was performed in the Renji dataset. All the error bars in the scatter plots represent SE.



*Bam*HI and *Xho*I (underlined), respectively. The DNA fragment obtained above was verified by sequencing and finally cloned into pCDNA3.1 between the *Bam*HI and *Xho*I sites to obtain pCDNA3.1-TMEFF2 $\Delta$ ID with Flag tag.

The DNA fragment encoding the SHP-1 gene (GenBank accession number NM\_080548) was amplified from human cDNA with the primers SHP-1F: 5'- AAGCTTA-TGCTGTCCCGTGGGTGG-3' and SHP-1R: 5'- CTCGAG-TCAGGCGTAATCAGGCACATCGTAAGGGTA-3', which introduced the cloning sites *Hind*III and *Xho*I (underlined), respectively. The cDNA fragment obtained above was verified by sequencing and finally cloned into pCDNA3.1 between the *Hind*III and *Xho*I sites to obtain pCDNA3.1-SHP-1WT with HA tag.

The SHP-1  $\Delta$ SH2D1,  $\Delta$ SH2D2, and  $\Delta$ PTPD DNA fragment was amplified from pCDNA3.1-SHP-1WT and the DNA fragments obtained above was verified by sequencing and finally cloned into pCDNA3.1 between the *Hind*III and *Xho*I sites to obtain pCDNA3.1-SHP-1 $\Delta$ SH2D1, pCDNA3.1-SHP-1 $\Delta$ SH2D2, and pCDNA3.1-SHP-1 $\Delta$ PTPD, with HA tag, respectively.

### In vivo experiments

To clarify the effect of TMEFF2 *in vivo*, 4-week-old male BALB/c nude mice obtained from Experimental Animal Centre of SIBS were used in our study. AGS cells ( $1.0 \times 10^7$ ) were injected subcutaneously into the right flank of these mice to establish the gastric cancer xenograft model. Ten days after subcutaneous inoculation, mice were randomly divided into 3 groups (8 mice/group) and were injected with PBS, or control adenoviruses, or TMEFF2 overexpression adenoviruses by ways of multipoint intratumoral injection every other day for 14 days. Tumor volume ( $\text{mm}^3$ ) was estimated by the formula: tumor volume ( $\text{mm}^3$ ) = shorter diameter<sup>2</sup>  $\times$  longer diameter/2. The tumor volumes data are presented as means  $\pm$  SE. All experimental procedures were approved by the Institutional Animal Care and Use Committee.

### Adenovirus and lentivirus transduction

The control adenovirus, TMEFF2 overexpression adenovirus, control shRNA lentivirus, and TMEFF2 shRNA lentivirus were all constructed by Shanghai SBO Medical Biotechnology Company.

### SupF mutation assay

The pSupFG1 plasmid and *E. coli* SY204 strain were kindly provided by Professor Gan Wang (Institute of Environmental Health Sciences, Wayne State University, Detroit, MI). As previously described (18, 19), a total of  $6 \times 10^5$  cells in 10 mL of culture medium were plated onto a 100-mm dish. After 16-hour cell culture, plasmid pSupFG1 (10  $\mu$ g) was transfected into the GES-1 cells or GES-1 with TMEFF2 depletion cells using Lipofectamine 2000 (Life Technologies) according to the supplier's recommendations. After 48 hours, propagated plasmids were extracted from the cells using a QIAprep Spin Miniprep Kit (Qiagen). The extracted plasmids were digested with *Dpn*I (Takara) to eliminate unreplicated plasmids, which retained a bacterial methylation pattern. After removal of proteins by phenol-chloroform extraction, DNA was purified with an Amicon Ultra-4 Centrifugal Filter Unit with Ultracel-30 membrane (Millipore, Billerica). The plasmid DNAs recovered were introduced into the *E. coli* SY204 (lacZ amber) with a Gene Pulser II electroporation apparatus (Bio-Rad). To select *E. coli* with a mutated *supF* gene, the transformed cells were plated onto a LB plate containing ampicillin, IPTG, and X-gal and were cultured at 37°C for 24 hours. As the *E. coli* SY204 strain carries an amber mutation in the lacZ gene, a functional *supF* gene suppresses the amber mutation in the lacZ gene and results in blue colonies on the X-gal plate whereas mutations in the *supF* reporter gene lead to colorless colonies on the X-gal plates. The mutation frequency of the *supF* reporter gene was determined as the number of mutant colonies to the number of total colonies on the plates.

### FISH assay

The FISH method was performed on slides with cells fixed in methanol/acetic acid. The *c-MYC* gene probe (Abnova) was purchased to detect the *c-MYC* gene alteration in the GES-1 cells and GES-1 cells with TMEFF2 depletion. The slides were washed in 2 $\times$  saline sodium citrate solution (SSC) and dehydrated in 70%, 80%, and 95% ethanol. The samples were then denatured with 70% formamide/2 $\times$  SSC (pH 7.0) at 70°C for 2 minutes and transferred to an iced ethanol (-20°C) series at 70%, 80%, and 95%. The probe was denatured at 96°C for 5 minutes. Then, 10  $\mu$ L was applied to the slide under a glass coverslip. *In situ* hybridization occurred at 42°C in a moist chamber overnight. Post-hybridization washings were done, and the nuclei

Figure 2. GO and GSEA in TMEFF2 higher/lower expression gastric cancer cells and patients. A, overview of the GO analysis used to identify the differential gene expression between TMEFF2 overexpression and control gastric cancer cells. B, GSEA comparing TMEFF2 lower expression group (red) against TMEFF2 higher expression group (blue) of patients with gastric cancer in the TCGA dataset, illustrating distinct pathways and biologic processes between both subgroups. Cytoscape and Enrichment map were used for visualization of the GSEA results (1% FDR,  $P = 0.005$ ). Nodes represent enriched gene sets, which are grouped and annotated by their similarity according to related gene sets. Enrichment results were mapped as a network of gene sets (nodes). Node size is proportional to the total number of genes within each gene set. Proportion of shared genes between gene sets is represented as the thickness of the green line between nodes. This network map was manually curated removing general and uninformative sub-networks, resulting in a simplified network map shown in B. Enrichment plots are shown for a set of activated genes related to cell proliferation and apoptosis and DNA damage in TCGA patients' dataset. The enrichment score (ES, green line) means the degree to which the gene set is overrepresented at the top or bottom of the ranked list of genes. Black bars indicate the position of genes belonging to the gene set in the ranked list of genes included in the analysis. A positive value indicates more correlation with "TMEFF2 lower expression" patients and a negative value indicates more correlation with "TMEFF2 higher expression" patients.

were counterstained with DAPI/antifade (Vector Laboratories). The molecular cytogenetic analysis was carried out under a ZEISS AXIOPHOT fluorescence microscope and an ISIS capture and image analysis system. For each sample, 200 interphase nuclei were analyzed.

### Bisulfite sequencing PCR analysis

The gDNA was extracted from the gastric tissues using QIAamp DNA Mini Kit (Qiagen). DNA was chemically modified with sodium metabisulphite. The bisulfite-modified DNA was PCR amplified with Pebp1-specific bisulphate sequencing primers (TMEFF2-BSP F1 5'-TGTTA-TAAGGAGGGAGTTTTGGGA-3'; and TMEFF2-BSP R1 5'-CTACATCTACTCCACCAATCAAAAC-3'; TMEFF2-BSP F2 5'-TGCGGGTAGTTTTATTTGAAGT-3'; and TMEFF2-BSP R2 5'-CGTTTAAAAACAAC AAATCCTCAAC-3'; SHP-1-BSP F 5'-AGGGTTGTGGTGAGAAATTAATTAG-3'; and SHP-1-BSP R 5'-TTACACACTCCAAACCCAAATAATAC-3'). The resulting PCR product was obtained by 1.5% agarose gel electrophoresis, cloned into pMD19-T vector (TaKaRa), and then 18 to 20 clones from the control and treated samples were sequenced.

Twenty-eight CpG sites spanning the -258 and +138 bp regions of *TMEFF2* gene promoter and 11 CpG sites spanning the -361 and -140 bp regions of *SHP-1* gene promoter were evaluated. Sequences were analyzed by using SeqScape software (Applied Biosystems) and Bioedit (<http://www.mbio.ncsu.edu/BioEdit/bioedit.html>).

### Statistical analysis

All statistical analyses were carried out using the program R ([www.r-project.org](http://www.r-project.org)) or SPSS for Windows 17.0.1 software (SPSS Inc.). Data from at least 3 independent experiments performed in triplicate are presented as the means  $\pm$  SE. Error bars in the scatter plots and the bar graphs represent SE. Data were examined whether they were normally distributed with the One-Sample Kolmogorov-Smirnov test. If the data were normally distributed, comparisons of measurement data between 2 groups were performed using the paired sample *t* test or independent sample *t* test and the comparisons among 3 or more groups were firstly performed by one-way ANOVA test. If the results showed significant difference, the Student Newman-Keuls analysis was used to test the difference between 2 groups. When the data were skewed distribution, comparisons were performed by nonparametric tests. Measurement data between 2 groups were performed using paired sample Wilcoxon signed rank test or nonparametric Mann-Whitney test. The measurement data among 3 or more groups were examined by Kruskal-Wallis test, and the differences between the 2 groups were further tested by Mann-Whitney test, adjusted for multiple comparisons using Bonferroni correction. Enumeration data were examined by  $\chi^2$  test or Fisher exact test. Overall survival in relation to *TMEFF2* or *SHP-1* expression was evaluated by the Kaplan-Meier survival curve and the Mantel-Cox test. The correlation of *TMEFF2*

and *SHP-1* expression was examined by Spearman correlation test. Statistical tests and *P* values were two-sided. Differences were considered significant with a value of *P* < 0.05.

## Results

### Integrative analysis reveals genes downregulated in gastric cancer tissues

To identify genes that are differentially expressed in gastric cancer at the genome scale, we compared the gene expression profiles of gastric cancer and normal gastric tissues through a microarray analysis. Using mRNA expression arrays containing approximately 27,958 best-defined human genes, we found that 5,417 genes were significantly altered in their expression: of which 2,584 genes were significantly downregulated in gastric cancer tissues (Supplementary Fig. S1A; raw data accessible via GEO number: GSE49052). Functional clustering analysis of the downregulated genes revealed a significant enrichment of genes (17%, 435/2,584 genes) related to cell proliferation, apoptosis, and cell cycle (Fig. 1A). Further analysis showed that 14 downregulated genes were specifically associated with cell proliferation, cell cycle, and apoptosis. Of these 14 genes, *RUNX3* and *IL1B* have been previously studied intensively in gastric cancer (20, 21). Of the remaining 12 genes, *TMEFF2* exhibited the most significantly decrease in transcriptional level in the microarray data. Furthermore, *TMEFF2* expression was significantly decreased in gastric cancer tissues when compared with the adjacent tissues of patients in Renji (from South of China), Jilin (from North of China), and TCGA independent dataset (Fig. 1B). To ensure that conclusions derived from these results are reliable, we have compared the *TMEFF2* expression between paired gastric cancer and normal tissues (*n* = 66) and tested for statistical significance by Student paired *t* test. Analysis of tumor/nontumor adjacent tissue (T/N) ratios for *TMEFF2* expression of 66 patients revealed that *TMEFF2* expression was decreased in approximately 70% gastric cancer patient tissues (*P* < 0.001, Fig. 1C). These results indicate that *TMEFF2* may play an important role in gastric carcinogenesis and therefore we chose to focus our experimental research on *TMEFF2*.

### Graded decrease in *TMEFF2* expression in gastric carcinogenesis correlates with gastric cancer patient survival

The real-time PCR data and immunohistochemical (IHC) staining showed that *TMEFF2* expression was gradually decreased from normal gastric tissue through to intestinal metaplasia, to dysplasia, and to gastric cancer (Supplementary Fig. S1B-S1D), suggesting that a decrease in *TMEFF2* expression is an early event in the multistep progression of gastric carcinogenesis.

Next, we explored whether the lower expression of *TMEFF2* in gastric cancer was associated with poor prognosis. Evaluation of *TMEFF2* expression in 105 patients with gastric cancer (Renji dataset) with different

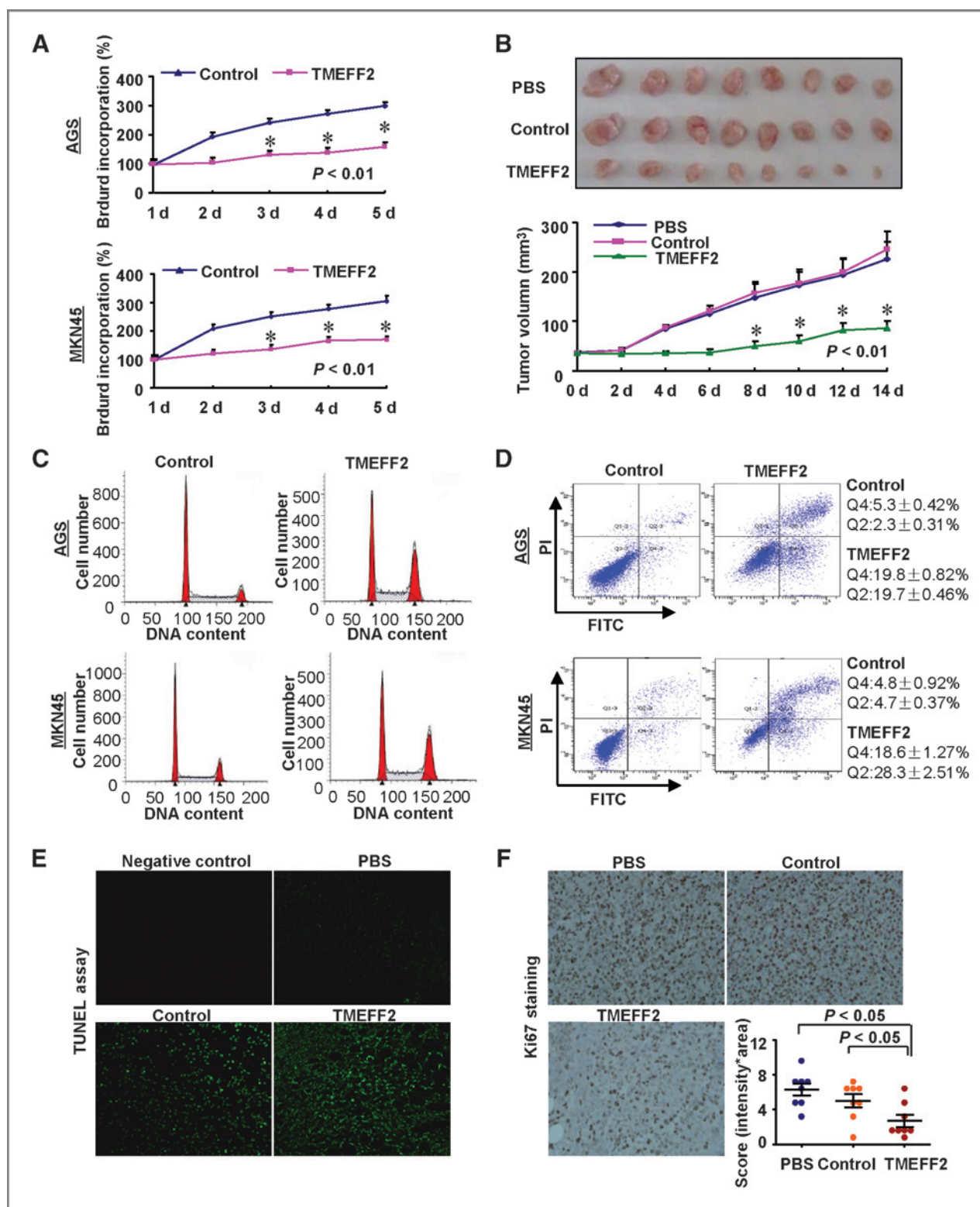
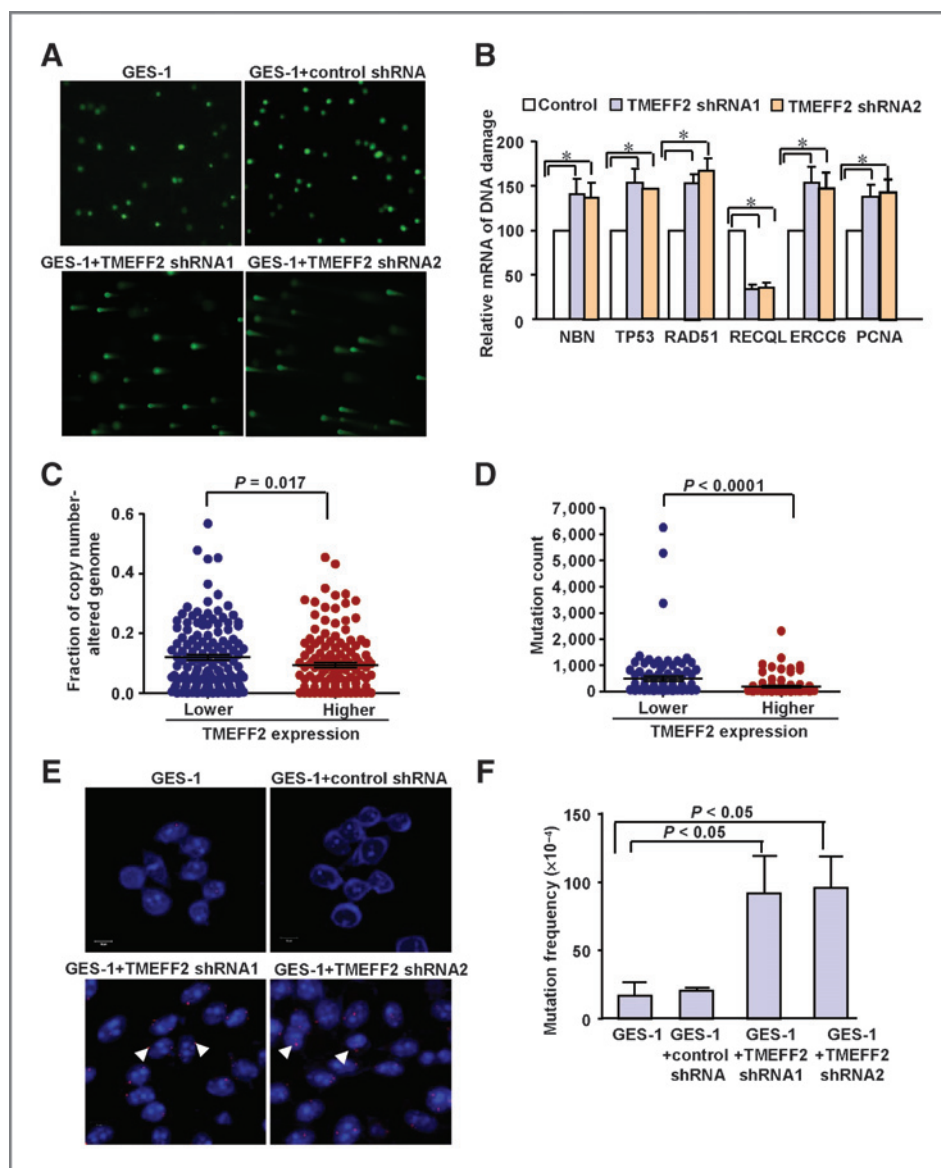


Figure 3. Functional roles of TMEFF2 *in vitro* and *in vivo*. A, TMEFF2 overexpression inhibited gastric cancer cell growth *in vitro*.  $n = 3$ ; \*,  $P < 0.01$ ; nonparametric Mann-Whitney test. B, representative data showed that overexpression of TMEFF2 significantly inhibited tumor growth in nude mice xenograft model. Tumor volume was measured after TMEFF2 overexpression adenoviruses treatments.  $n = 8$ ; \*,  $P < 0.01$ ; nonparametric Mann-Whitney test. C, cell-cycle arrest after TMEFF2 overexpression in AGS and MKN45 gastric cancer cells was assessed by flow cytometry.  $n = 3$ . D, cell apoptosis after TMEFF2 overexpression in AGS and MKN45 gastric cancer cells was assessed by flow cytometry.  $n = 3$ . E, higher percentage of apoptotic cells in TMEFF2 overexpression group tumors was detected compared with PBS or control groups by the TUNEL reaction.  $n = 8$ . F, IHC staining of Ki67 of the 3 group xenografts was shown.  $n = 3$ ;  $P < 0.05$ ; independent sample *t* test. Error bars in the scatter plots represent SE.



**Figure 4.** Detection of the genomic instability and DNA mutation frequency in GES-1 cells with TMEFF2 depletion. **A**, representative images for comet assay in GES-1 cells after introduction of control shRNA and TMEFF2 shRNA virus.  $n = 3$ . **B**, the mRNA levels of DNA damage-related genes were measured in GES-1 cells after introduction of control shRNA and TMEFF2 shRNA virus.  $n = 3$ ; \*,  $P < 0.05$ . **C** and **D**, genome instability (DNA copy number alteration and mutation) was detected in TCGA patients with gastric cancer with TMEFF2 lower expression ( $P < 0.05$ ; nonparametric Mann-Whitney test). Error bars in the scatter plots represent SE. **E**, the immunofluorescence data revealed that more DNA copies of *c-MYC* gene were detected in GES-1 cells with TMEFF2 stable knockdown. (The FISH probe of *c-MYC* is labeled with Texas Red.) **F**, TMEFF2 depletion significantly increased the *supF*-mutant frequencies in GES-1 cells.  $n = 3$ ;  $P < 0.01$ ; independent sample *t* test. Error bars in the scatter plots represent SE.

clinopathologic features revealed that the TMEFF2 expression was negatively correlated with the histologic stage ( $P < 0.001$ ; Supplementary Table S3) and tumor size ( $P < 0.05$ , Fig. 1D). No correlation was found between TMEFF2 expression and other clinicopathologic features. We also compared the survival time in patients of Renji dataset. The cumulative survival rate was significantly higher in patients with higher TMEFF2-expressing tumors than in those with lower TMEFF2-expressing tumors [ $P = 0.0148$ ; HR, 0.57; 95% confidence interval (CI), 0.37–0.90; Fig. 1E]. In addition, multivariate analysis revealed that the lower expression of TMEFF2 was found to be significantly associated with poor survival in patients with gastric cancer independently of the TNM stage ( $P = 0.016$ ; Fig. 1F). These data indicate that TMEFF2 expression could represent a new prognostic factor in patients with gastric cancer.

### Functional roles of TMEFF2 as a tumor suppressor *in vitro* and *in vivo*

To elucidate whether TMEFF2 could play a role in preventing gastric cancer occurrence, a microarray analysis was performed to compare the gene expression profiles of TMEFF2 and control plasmid transfectants. A total of 1,442 downregulated genes ( $\geq 2$ -fold) and 1,395 upregulated genes ( $\geq 2$ -fold) was detected (raw data accessible via GEO number: GES49052) after overexpression of TMEFF2 in gastric cancer cells. Gene Ontology analysis revealed changes in gene sets related to cell proliferation, apoptosis, and DNA damage in TMEFF2-overexpressing cells (Fig. 2A). To gain further insight into the biologic pathways involved in gastric cancer pathogenesis stratified by the median of TMEFF2 expression level, GSEA analysis was performed in TCGA and Jilin datasets. Enrichment plots of GSEA showed that the gene signatures of cell

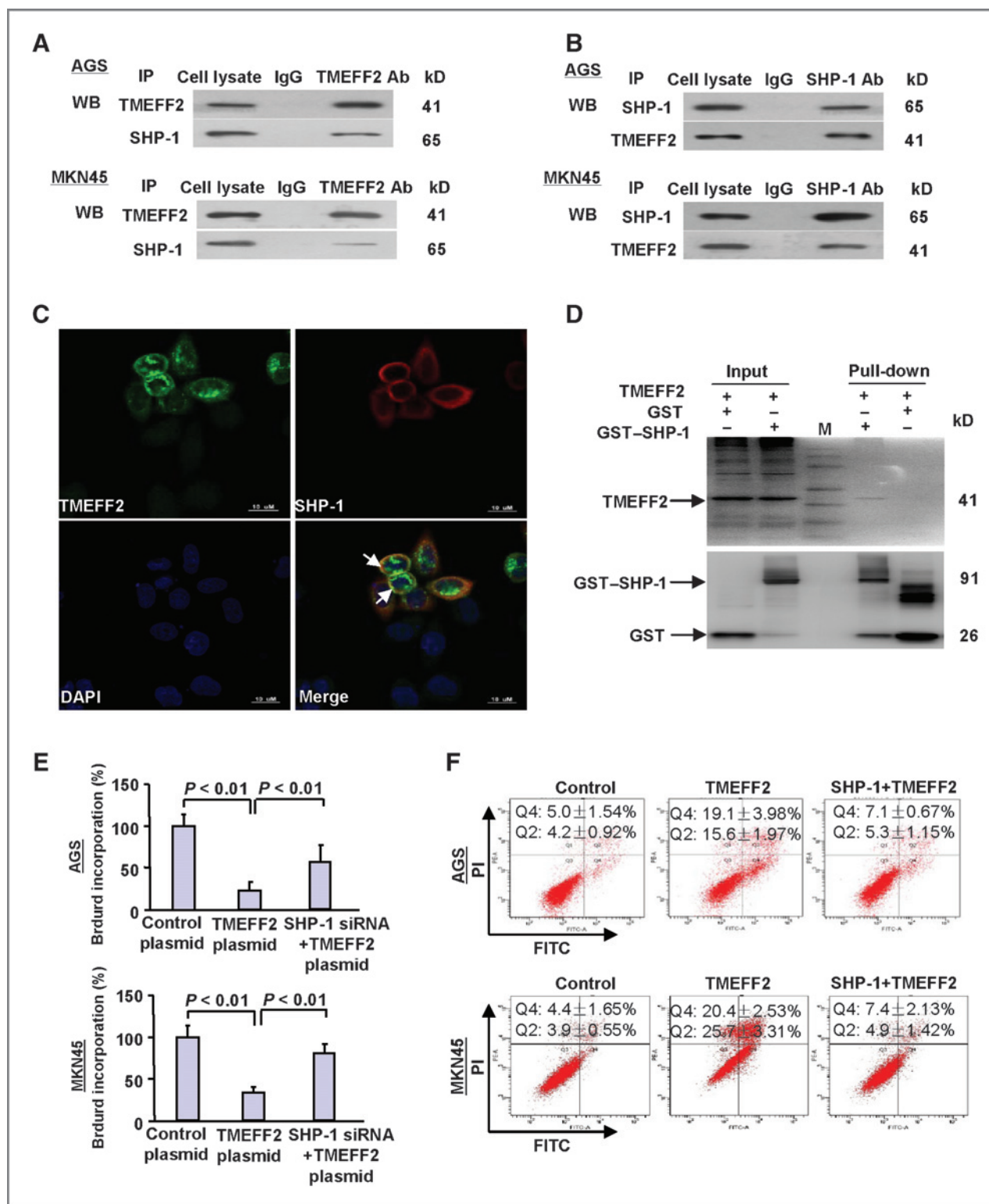


Figure 5. TMEFF2 binds to SHP-1 *in vitro* and *in vivo*. A and B, Co-IP showed that TMEFF2 interacts with SHP-1 in the gastric cancer cell lines AGS and MKN45.  $n = 3$ . C, immunofluorescence revealed that TMEFF2 is colocalized with SHP-1.  $n = 3$ . D, TMEFF2 was pulled down by GST/SHP-1 fusion protein, but not by GST alone.  $n = 3$ . E and F, downregulation of SHP-1 dramatically blocked TMEFF2-induced decrease in cell proliferation and increase in cell apoptosis in gastric cancer cell lines AGS and MKN45.  $n = 3$ ; nonparametric Mann-Whitney test. Control plasmid: pCDNA3.1; TMEFF2 plasmid: pCDNA3.1-TMEFF2WT.

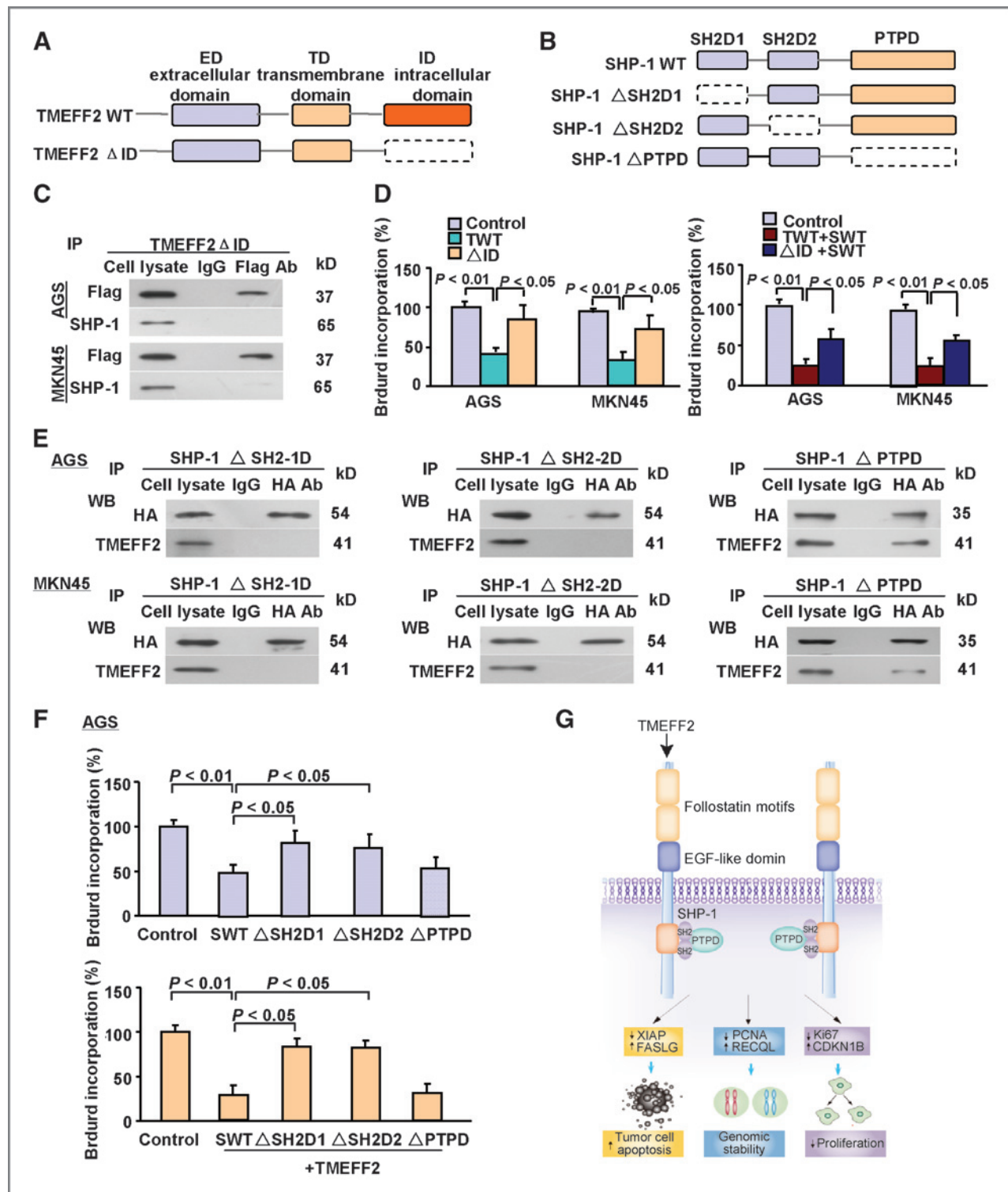


Figure 6. TMEFF2 functions through its intracellular domain that associates with the 2 SH2 domains of SHP-1. A, schematic representation of TMEFF2 protein and the truncated mutant. TMEFF2 protein includes the extracellular domain (ED in pale blue), the transmembrane domain (TD in tan), and the intracellular domain (ID in orange). The TMEFF2 mutant without the ID was named as TMEFF2 $\Delta$ ID. B, schematic representation of SHP-1 protein and the truncated mutants. SHP-1 protein includes the SH2 domain-1/2 (SH2D1 and SH2D2 in pale blue) and the protein tyrosine phosphatase (PTP) domain (PTPD in tan). The SHP-1 mutant without the SH2D1, SH2D2, or PTPD was named as SHP-1 $\Delta$ SH2D1,  $\Delta$ SH2D2, or  $\Delta$ PTPD, respectively. C, Co-IP was performed after coexpression of TMEFF2 $\Delta$ ID with Flag tag and SHP-1 in AGS and MKN45 cells.  $n = 3$ . D, cell proliferation assays were performed in gastric cancer cells after overexpression of TMEFF2WT/ $\Delta$ ID with or without SWT.  $n = 3$ ; nonparametric Mann-Whitney test. (Continued on the following page.)

proliferation and apoptosis were more correlated with patients with TMEFF2 lower expression versus patients with TMEFF2 higher expression in the both individual datasets (Fig. 2B and Supplementary Fig. S2A–S2C). The top-scoring genes recurring in the 2 pathways included key cancer genes, such as CDKN1B (p27), Ki67, and FASLG. Further real-time PCR data confirmed that alteration of TMEFF2 expression dramatically affected the key gene signatures which are involved in tumorigenesis (Supplementary Fig. S3), suggesting that TMEFF2 may be a key regulator in gastric tumorigenesis.

To validate the GSEA analysis of TMEFF2, we transfected TMEFF2-overexpressing plasmid into the gastric cancer cell lines AGS and MKN45. Both these cell lines display a lower expression of TMEFF2 than GES-1 gastric cells (Supplementary Fig. S4A and S4B). Overexpression of TMEFF2 significantly inhibited gastric cancer cell proliferation both *in vitro* and *in vivo* (Fig. 3A and B; Supplementary Fig. S4C). We also examined the effects of TMEFF2 on gastric cancer cell-cycle progression and apoptosis. As illustrated in Fig. 3C, overexpression of TMEFF2 dramatically blocked the cell cycle at the G<sub>2</sub>–M phase. In addition, apoptotic gastric cancer cells were significantly increased after overexpression of TMEFF2 both *in vitro* and *in vivo* (Fig. 3D and E). Furthermore, the knockdown of TMEFF2 significantly increased cell proliferation in GES-1 cells (Supplementary Fig. S4D). These data suggest that TMEFF2 may function as a tumor suppressor in gastric cancer through inhibition of cell-cycle progression and the induction of cell apoptosis. IHC staining and Western blot analyses showed that alteration of TMEFF2 expression significantly changed the expression of the cell proliferation markers Ki67 and proliferating cell nuclear antigen (PCNA) in gastric cells (Fig. 3F and Supplementary Fig. S4E and S4F). In addition, P27 and FASL (a trigger of apoptosis) were also upregulated following TMEFF2 overexpression (Supplementary Fig. S4E). The data were consistent with the correlation of TMEFF2 with clinicopathologic features (especially tumor size) and GSEA analysis in gastric cancer.

#### Knockdown of TMEFF2 significantly increased DNA damage, genomic instability, and DNA mutation frequency in GES-1 cells

According to the GSEA, DNA damage-related genes were active in patients with TMEFF2 lower expression (Fig. 2B), we next performed functional assay to validate that. The representative data of comet assay showed that knockdown of TMEFF2 significantly increased DNA damage (Fig. 4A) and induced the alteration of DNA damage-related gene signatures in GES-1 cells (Fig. 4B), indicating

that knockdown of TMEFF2 may induce DNA damage in GES-1 cells.

Moreover, in TCGA dataset, we found that a greater fraction of copy number altered genome and DNA mutations were detected in patients with gastric cancer with lower TMEFF2 expression than in those with higher TMEFF2 expression (Fig. 4C and D). To explore the role of TMEFF2 in gastric genome stability, we introduced TMEFF2 shRNA lentivirus into GES-1 cells. As *c-MYC* gene amplification was often detected in gastric carcinogenesis (22, 23), we detected the *c-MYC* gene amplification in GES-1 with TMEFF2-depleted cells by FISH assay. More DNA copies of *c-MYC* gene were detected in the GES-1 cells after stable knockdown of TMEFF2 (Fig. 4E), suggesting that downregulation of TMEFF2 may increase genome instability via accumulating of extra copies of DNA in GES-1 cells.

Furthermore, *supF* mutation assay showed that replication of the pSupFG1 vector in GES-1 cells with stable knockdown of TMEFF2 yielded a significantly higher (5-fold) mutant frequency than in the control shRNA cells (TMEFF2 shRNA1 vs. control:  $91 \pm 16 \times 10^{-4}$  vs.  $20 \pm 1 \times 10^{-4}$ ,  $P = 0.011$ ; TMEFF2 shRNA2 vs. control:  $96 \pm 13 \times 10^{-4}$  vs.  $20 \pm 1 \times 10^{-4}$ ,  $P = 0.005$ ; Fig. 4F), indicating that the DNA mutation is more frequent in TMEFF2-depleted gastric cells than in normal gastric cells. The data are consistent with our DNA mutation statistic data in patients.

#### Association of TMEFF2 with SHP-1

To dissect the molecular mechanism of the TMEFF2-induced inhibition of gastric cancer cell growth, we used the LC/MS-based proteomic approach to identify protein candidates that functionally associate with TMEFF2. The details of LC/MS identification were shown in Supplementary Table S4. Interestingly, 6 peptide fragments of protein tyrosine phosphatase SHP-1 were identified in TMEFF2 pull-down complex as the main fraction. SHP-1 functions as an important regulator of multiple signaling pathways in hematopoietic cells and in tumorigenesis (24, 25). We explored further the nature of the interaction between SHP-1 and TMEFF2. Co-IP experiments in AGS and MKN45 cells confirmed the SHP-1/TMEFF2 interaction (Fig. 5A and B). In addition, immunofluorescence revealed that TMEFF2 is colocalized with SHP-1 (Fig. 5C). Figure 5A–C shows the *in vivo* data. Second, as shown in Fig. 5D, TMEFF2 was pulled down by the GST/SHP-1 fusion protein but not by GST alone, suggesting that TMEFF2 may directly interact with SHP-1 (*in vitro* data). The results obtained from LC/MS-based proteomic screening combined with a variety of biologic approaches indicate that SHP-1 directly interacts with TMEFF2.

(Continued.) TWT: TMEFF2WT; SWT: SHP-1WT. E, Co-IP was performed after coexpression of SHP-1 $\Delta$ SH2D1/ $\Delta$ SH2D2/ $\Delta$ PTPD with HA tag and TMEFF2 WT in gastric cancer cells.  $n = 3$ . F, cell proliferation assays were performed in AGS cells after overexpression of SHP-1WT/ $\Delta$ SH2D1/ $\Delta$ SH2D2/ $\Delta$ PTPD or these constructs combined with TMEFF2;  $n = 3$ ; nonparametric Mann–Whitney test. G, schematic representation of the biologic role of TMEFF2 in gastric carcinogenesis. TMEFF2 may act as a tumor suppressor by regulating cell proliferation, apoptosis, and genomic stability in gastric carcinogenesis. TMEFF2 directly interacts with SHP-1 via its intercellular domain. The SH2 1/2 domains of SHP-1 are important for its interaction with TMEFF2 and the tumor-suppressive function of TMEFF2.

We next detected whether SHP-1 mediates the biologic function of TMEFF2 in gastric cancer. The functional assay showed that the downregulation of SHP-1 markedly blocked the TMEFF2-induced decrease in cell proliferation and increase in cell apoptosis (Fig. 5E and F), indicating that SHP-1 may mediate the function of TMEFF2 in gastric cancer.

#### TMEFF2 functions through its association with SHP-1

To explore the mechanism of SHP-1-mediated TMEFF2 function in gastric cancer, we sought to identify regions within TMEFF2 and SHP-1 that are important for SHP-1/TMEFF2 interaction. The human TMEFF2 protein contains an extracellular domain (residues 41–320), a transmembrane domain (residues 321–341), and an intracellular domain (residues 342–374; Fig. 6A). The human SHP-1 protein contains 2 SH2 domains (SH2D1 and SH2D2; residues 4–100 and 110–213, respectively) and a protein tyrosine phosphatase domain (PTPD; residues 244–515; Fig. 6B). To determine the regions of TMEFF2 and SHP-1 responsible for their physical interaction, we generated a truncation mutant of the TMEFF2 intracellular domain (termed TMEFF2 $\Delta$ ID), with a Flag tag and truncation mutants of SHP-1, namely  $\Delta$ SH2D1,  $\Delta$ SH2D2, and  $\Delta$ PTPD, with an HA tag. All the truncation mutants were successfully overexpressed in gastric cancer cells (Supplementary Fig. S4G and S4H). Deletion of the intracellular domain significantly blocked the interaction between TMEFF2 and SHP-1 in a Co-IP assay (Fig. 6C) as well as the TMEFF2-mediated loss of cell proliferation in gastric cancer cells (Fig. 6D), suggesting that the TMEFF2 $\Delta$ ID domain is important for the TMEFF2/SHP-1 interaction and TMEFF2 function in gastric cancer.

In addition, deletion of the SH2D1 or SH2D2 domain, but not deletion of the PTP domain, significantly blocked TMEFF2/SHP-1 interaction (Fig. 6E) as determined through a Co-IP assay, indicating that the 2 SH2 domains of SHP-1 are required for the interaction between TMEFF2 and SHP-1. A further functional assay showed that the overexpression of SHP-1 $\Delta$ SH2D1 or  $\Delta$ SH2D2, but not  $\Delta$ PTPD, significantly blocked the TMEFF2-induced loss of cell proliferation (Fig. 6F and Supplementary Fig. S5A). These data are consistent with the Co-IP data and suggest that the 2 SH2 domains of SHP-1 are important for the tumor-suppressive function of TMEFF2 in gastric cancer.

We also analyzed the somatic mutation data of TCGA (320 cases) and Renji datasets (20 cases; Supplementary Table S5). However, no DNA mutations in the intracellular domain of TMEFF2 and in the SH2D1, SH2D2, or PTPD domains of SHP-1 were observed, indicating that somatic mutation of TMEFF2 may not be the major cause of deregulation of this gene in gastric carcinogenesis.

#### Correlation of TMEFF2 and SHP-1 expression in human gastric cancer

Because it is important to fully clarify the roles of SHP-1 on the function of TMEFF2 *in vivo*, we further tested the correlation of TMEFF2 and SHP-1 in human gastric mucosal

specimens. Similar to TMEFF2, SHP-1 expression was also significantly decreased from normal tissues to precancerous lesions to cancer (Supplementary Fig. S6A). The correlation analysis showed that TMEFF2 expression was significantly correlated with SHP-1 in gastric carcinogenesis ( $r_{\text{Spearman}} = 0.479$ ,  $P < 0.01$ ; Supplementary Fig. S6B).

Moreover, to test the possibility that inhibition of the tumor-suppressive function of TMEFF2 (and associated SHP-1) could be through an increase in the methylation level of TMEFF2 and SHP-1 gene promoters, we analyzed the gene promoter methylation patterns of the relevant gene promoters using bisulfite sequencing PCR (BSP) analysis (26). The promoter methylation levels of TMEFF2 and SHP-1 were gradually increased from normal gastric tissue, intestinal metaplasia, dysplasia through to gastric cancer (Supplementary Fig. S6C), suggesting that the synchronous expression of SHP-1 and TMEFF2 may be regulated by methylation in gastric cancer development.

Importantly, the cumulative survival rate was significantly better in patients with higher SHP-1-expressing tumors than in those with lower SHP-1-expressing tumors ( $P = 0.031$ ; HR, 0.62; 95% CI, 0.41–0.96; Supplementary Fig. S6D), indicating that SHP-1 downregulation is also significantly associated with poor survival in gastric cancer. We further investigated the survival difference in patients with gastric cancer with combined higher/lower expressions of TMEFF2 and SHP-1. The prognosis is better in patients with higher expression levels of both TMEFF2 and SHP-1 (TMEFF2<sup>H</sup> + SHP-1<sup>H</sup>) than in patients with lower expression levels of both TMEFF2 and SHP-1 (TMEFF2<sup>L</sup> + SHP-1<sup>L</sup>;  $P = 0.0039$ ; HR, 0.45; 95% CI, 0.26–0.78; Supplementary Fig. S6E), indicating that higher levels of TMEFF2 and SHP-1 may predict better overall survival in patients with gastric cancer.

#### Discussion

The deregulation of TMEFF2 has been demonstrated in various tumor types (10, 12, 27). However, the biologic functions and clinical implication of TMEFF2 in gastric cancer remain unknown. In the present study, we highlight a functional role for TMEFF2 in gastric carcinogenesis.

We compared TMEFF2 expression between gastric cancer tissues and adjacent nontumor tissues in relation to gastric cancer pathogenesis in Renji, Jilin, and TCGA datasets. TMEFF2 expression is significantly decreased in gastric cancer tissues when compared with adjacent tissues in the 3 individual datasets, and the expression of TMEFF2 is higher in male patients than in female patients. It is possible that the expression of TMEFF2 may be associated with hormone metabolism and is strongly associated with androgen. Our data are consistent with previous report that TMEFF2 is initially identified as an androgen-regulated gene in prostate cancer cells and is regulated by androgens (10). Recently, another group also illustrated that androgen may regulate the translation of TMEFF2 in prostate cancer via promoting the phosphorylation level of eIF2 $\alpha$  (28). In addition, TMEFF2 is progressively downregulated from

normal gastric tissues through to precancerous tissues to gastric cancer tissues, and TMEFF2 higher expression in gastric cancer is associated with a favorable prognosis. Moreover, the downregulation of TMEFF2 in gastric cancer was found to be negatively correlated with the histologic grade and tumor size. These data suggest that TMEFF2 may play important roles in gastric cancer.

GO analysis and GSEA demonstrated that the cell proliferation, apoptosis, and DNA repair pathways were significantly enriched in response to TMEFF2 alteration in gastric cancer cells and patients. The bioinformatics analyses were further validated in the subsequently performed *in vitro* and *in vivo* experiments. In cultured gastric cancer cells and xenograft mouse models, TMEFF2 markedly suppressed cell growth through induction of cell-cycle arrest and increase of cell apoptosis. Moreover, TMEFF2 may participate in maintaining gastric genomic stability, as greater numbers of extra copies of DNA and frequently DNA mutation were detected in normal gastric cells and patients with TMEFF2 depletion. These data consistently indicate that aggressive gastric cancer cells are addicted to lower TMEFF2 expression, which explains the important role that TMEFF2 plays in the progression of gastric cancer. Although TMEFF2 has been reported to mediate tumor suppression in colorectal cancer (29), this study provides the first demonstration of its crucial functions in gastric cancer development by combining high-throughput data analysis and functional assays. The strong correlation between TMEFF2 expression and gastric cancer patient survival, tumor size, and pathologic stage highlights the potential value of TMEFF2 as a novel biomarker for gastric cancer prognosis.

Several studies have indicated that TMEFF2 is a tumor-suppressor in human cancer cells (11–13), whereas others reports have demonstrated that the elevated TMEFF2 expression is associated with higher prostate cancer grade and hormone independence (9, 30). Truncated TMEFF2 (without the cytoplasmic domain) may promote cell proliferation through the induction of ERK1/2 phosphorylation (14). Therefore, the role of TMEFF2 in carcinogenesis requires further study.

The TMEFF2 protein has been found to interact with multiple proteins. In prostate cancer cells, TMEFF2 binds to sarcosine dehydrogenase (SARDH) and modulates cellular sarcosine levels (31). It has been suggested that TMEFF2 and SARDH may cooperate to modulate one-carbon metabolism and invasion in cancer cells (32). The extracellular domain of TMEFF2 interacts with platelet-derived growth factor (PDGF)-AA and regulates PDGF signaling (12). In this study, using a combination of MS analysis, confocal microscopy, and immunoprecipitation assays, we reveal that TMEFF2 directly binds to the SH2 domains of SHP-1. Importantly, we show that the intracellular domain of TMEFF2 mediates the TMEFF2/SHP-1 interaction and the TMEFF2-mediated decrease in cell proliferation in gastric cancer. The tumor-suppressive function of TMEFF2 is mediated by SHP-1, particularly the SH2 domains of SHP-1. SHP-1 is primarily expressed in hematopoietic cells and behaves as a key regulator

of the intracellular phosphotyrosine levels in lymphocytes (33, 34). SHP-1 regulates the intracellular signaling of different transmembrane receptors, including growth factor receptors and cytokine receptors. For example, decreased or abolished SHP-1 expression or activity results in increased JAK kinase activity and can directly cause abnormal cell growth (35, 36). SHP-1 has therefore been considered a tumor suppressor in different cancers.

The clinical relevance of the interaction of TMEFF2 and SHP-1 was further supported by the analysis of human tissues along the gastric carcinogenic cascade. The expression of TMEFF2 was positively correlated with that of SHP-1 in human precancerous lesions and gastric cancer. Furthermore, higher expressions of TMEFF2 and SHP-1 cases exhibited the best prognosis. The synchronous expression of SHP-1 and TMEFF2 may be regulated by methylation of their gene promoters during gastric cancer development.

In conclusion, our findings have provided additional insight into the mechanisms of gastric carcinogenesis. As represented in Supplementary Fig. S6G, TMEFF2 may play an important role in the progression of gastric tumorigenesis and it is identified as a potential biomarker and therapeutic target for gastric cancer.

#### Disclosure of Potential Conflicts of Interest

No potential conflicts of interest were disclosed.

#### Authors' Contributions

**Conception and design:** T. Sun, W. Du, H. Xiong, J. Hong

**Development of methodology:** W. Zou, H. Chen

**Acquisition of data (provided animals, acquired and managed patients, provided facilities, etc.):** Y. Yu, Y. Weng, L. Ren, H. Zhao, Y. Wang, Y. Chen, J. Xu, Y. Xiang, W. Qin

**Analysis and interpretation of data (e.g., statistical analysis, biostatistics, computational analysis):** T. Sun, W. Du, H. Xiong

**Writing, review, and/or revision of the manuscript:** T. Sun, W. Du, H. Chen, J. Hong

**Administrative, technical, or material support (i.e., reporting or organizing data, constructing databases):** W. Cao, W. Zou, H. Chen

**Study supervision:** J. Fang

#### Acknowledgments

The authors thank Dr. Gan Wang of the Institute of Environmental Health Sciences, Wayne State University, for providing us with the pSupFG1 plasmid and *E. coli* SY204 strain.

#### Grant Support

This work was supported by grants from National Basic Research Program of China 973 program (grant no. 2010CB5293), the National High Technology Research and Development Program of China (863 Program Grant No. 2012AA02A504), the National Natural Science Foundation (grant no. 30921140311) to J. Fang; the grant from the National Natural Science Foundation (no. 91129724), National Natural Science Foundation (no. 31271366), Shanghai Rising-Star Program (no. 12QA1402000) and The Program for Professor of Special Appointment (Eastern Scholar) at Shanghai Institutions of Higher Learning (no. 201268) to J. Hong; the grant from the National Natural Science Foundation (no. 81270480) to H. Xiong; the grant from the National Natural Science Foundation (nos. 81301713 and 31271501) to W. Du and Y. Chen.

The costs of publication of this article were defrayed in part by the payment of page charges. This article must therefore be hereby marked *advertisement* in accordance with 18 U.S.C. Section 1734 solely to indicate this fact.

Received February 5, 2014; revised May 1, 2014; accepted May 20, 2014; published OnlineFirst July 1, 2014.

## References

1. Jemal A, Bray F, Center MM, Ferlay J, Ward E, Forman D. Global cancer statistics. *CA Cancer J Clin* 2011;61:69–90.
2. Ueda T, Volinia S, Okumura H, Shimizu M, Taccioli C, Rossi S, et al. Relation between microRNA expression and progression and prognosis of gastric cancer: a microRNA expression analysis. *Lancet Oncol* 2010;11:136–46.
3. Cunningham D, Allum WH, Stenning SP, Thompson JN, Van de Velde CJ, Nicolson M, et al. Perioperative chemotherapy versus surgery alone for resectable gastroesophageal cancer. *N Engl J Med* 2006;355:11–20.
4. Cheng AS, Li MS, Kang W, Cheng VY, Chou JL, Lau SS, et al. Helicobacter pylori causes epigenetic dysregulation of FOXD3 to promote gastric carcinogenesis. *Gastroenterology* 2013;144:122–33.e9.
5. Jenkins BJ, Grail D, Nheu T, Najdovska M, Wang B, Waring P, et al. Hyperactivation of Stat3 in gp130 mutant mice promotes gastric hyperproliferation and desensitizes TGF- $\beta$  signaling. *Nat Med* 2005;11:845–52.
6. Palanisamy N, Ateeq B, Kalyana-Sundaram S, Pflueger D, Ramnarayanan K, Shankar S, et al. Rearrangements of the RAF kinase pathway in prostate cancer, gastric cancer and melanoma. *Nat Med* 2010;16:793–8.
7. Horie M, Mitsumoto Y, Kyushiki H, Kanemoto N, Watanabe A, Taniguchi Y, et al. Identification and characterization of TMEFF2, a novel survival factor for hippocampal and mesencephalic neurons. *Genomics* 2000;67:146–52.
8. Heanue TA, Pachnis V. Expression profiling the developing mammalian enteric nervous system identifies marker and candidate Hirschsprung disease genes. *Proc Natl Acad Sci U S A* 2006;103:6919–24.
9. Afar DE, Bhaskar V, Ibsen E, Breinberg D, Henshall SM, Kench JG, et al. Preclinical validation of anti-TMEFF2-auristatin E-conjugated antibodies in the treatment of prostate cancer. *Mol Cancer Ther* 2004;3:921–32.
10. Gery S, Sawyers CL, Agus DB, Said JW, Koeffler HP. TMEFF2 is an androgen-regulated gene exhibiting antiproliferative effects in prostate cancer cells. *Oncogene* 2002;21:4739–46.
11. Philipp AB, Stieber P, Nagel D, Neumann J, Spelsberg F, Jung A, et al. Prognostic role of methylated free circulating DNA in colorectal cancer. *Int J Cancer* 2012;131:2308–19.
12. Lin K, Taylor JR Jr, Wu TD, Gutierrez J, Elliott JM, Vernes JM, et al. TMEFF2 is a PDGF-AA binding protein with methylation-associated gene silencing in multiple cancer types including glioma. *PLoS ONE* 2011;6:e18608.
13. Costa VL, Henrique R, Danielsen SA, Duarte-Pereira S, Eknaes M, Skotheim RI, et al. Three epigenetic biomarkers, GDF15, TMEFF2, and VIM, accurately predict bladder cancer from DNA-based analyses of urine samples. *Clin Cancer Res* 2010;16:5842–51.
14. Ali N, Knauper V. Phorbol ester-induced shedding of the prostate cancer marker transmembrane protein with epidermal growth factor and two follistatin motifs 2 is mediated by the disintegrin and metalloproteinase-17. *J Biol Chem* 2007;282:37378–88.
15. Xiong H, Hong J, Du W, Lin YW, Ren LL, Wang YC, et al. Roles of STAT3 and ZEB1 proteins in E-cadherin down-regulation and human colorectal cancer epithelial-mesenchymal transition. *J Biol Chem* 2012;287:5819–32.
16. Shevchenko A, Tomas H, Havlis J, Olsen JV, Mann M. In-gel digestion for mass spectrometric characterization of proteins and proteomes. *Nat Protoc* 2006;1:2856–60.
17. Uyama N, Zhao L, Van Rossen E, Hirako Y, Reynaert H, Adams DH, et al. Hepatic stellate cells express synemin, a protein bridging intermediate filaments to focal adhesions. *Gut* 2006;55:1276–89.
18. Wang G, Levy DD, Seidman MM, Glazer PM. Targeted mutagenesis in mammalian cells mediated by intracellular triple helix formation. *Mol Cell Biol* 1995;15:1759–68.
19. Chen Z, Xu XS, Yang J, Wang G. Defining the function of XPC protein in psoralen and cisplatin-mediated DNA repair and mutagenesis. *Carcinogenesis* 2003;24:1111–21.
20. Huang FY, Chan AO, Rashid A, Wong DK, Cho CH, Yuen MF. Helicobacter pylori induces promoter methylation of E-cadherin via interleukin-1 $\beta$  activation of nitric oxide production in gastric cancer cells. *Cancer* 2012;118:4969–80.
21. Liu Z, Xu X, Chen L, Li W, Sun Y, Zeng J, et al. Helicobacter pylori CagA inhibits the expression of Runx3 via Src/MEK/ERK and p38 MAPK pathways in gastric epithelial cell. *J Cell Biochem* 2012;113:1080–6.
22. Hara T, Ooi A, Kobayashi M, Mai M, Yanagihara K, Nakanishi I. Amplification of c-myc, K-sam, and c-met in gastric cancers: detection by fluorescence in situ hybridization. *Lab Invest* 1998;78:1143–53.
23. Sakakura C, Mori T, Sakabe T, Ariyama Y, Shinomiya T, Date K, et al. Gains, losses, and amplifications of genomic materials in primary gastric cancers analyzed by comparative genomic hybridization. *Genes Chromosomes Cancer* 1999;24:299–305.
24. Paling NR, Welham MJ. Tyrosine phosphatase SHP-1 acts at different stages of development to regulate hematopoiesis. *Blood* 2005;105:4290–7.
25. Wu C, Sun M, Liu L, Zhou GW. The function of the protein tyrosine phosphatase SHP-1 in cancer. *Gene* 2003;306:1–12.
26. Li LC, Dahiya R. MethPrimer: designing primers for methylation PCRs. *Bioinformatics* 2002;18:1427–31.
27. Tsunoda S, Smith E, De Young NJ, Wang X, Tian ZQ, Liu JF, et al. Methylation of CLDN6, FBN2, RBP1, RBP4, TFPI2, and TMEFF2 in esophageal squamous cell carcinoma. *Oncol Rep* 2009;21:1067–73.
28. Overcash RF, Chappell VA, Green T, Geyer CB, Asch AS, Ruiz-Echevarria MJ. Androgen signaling promotes translation of TMEFF2 in prostate cancer cells via phosphorylation of the alpha subunit of the translation initiation factor 2. *PLoS ONE* 2013;8:e55257.
29. Elahi A, Zhang L, Yeatman TJ, Gery S, Sebti S, Shibata D. HPP1-mediated tumor suppression requires activation of STAT1 pathways. *Int J Cancer* 2008;122:1567–72.
30. Mohler JL, Morris TL, Ford OH III, Alvey RF, Sakamoto C, Gregory CW. Identification of differentially expressed genes associated with androgen-independent growth of prostate cancer. *Prostate* 2002;51:247–55.
31. Chen X, Overcash R, Green T, Hoffman D, Asch AS, Ruiz-Echevarria MJ. The tumor suppressor activity of the transmembrane protein with epidermal growth factor and two follistatin motifs 2 (TMEFF2) correlates with its ability to modulate sarcosine levels. *J Biol Chem* 2011;286:16091–100.
32. Green T, Chen X, Ryan S, Asch AS, Ruiz-Echevarria MJ. TMEFF2 and SARDH cooperate to modulate one-carbon metabolism and invasion of prostate cancer cells. *Prostate* 2013;73:1561–75.
33. Sen G, Bikah G, Venkataraman C, Bondada S. Negative regulation of antigen receptor-mediated signaling by constitutive association of CD5 with the SHP-1 protein tyrosine phosphatase in B-1 B cells. *Eur J Immunol* 1999;29:3319–28.
34. Bruecher-Encke B, Griffin JD, Neel BG, Lorenz U. Role of the tyrosine phosphatase SHP-1 in K562 cell differentiation. *Leukemia* 2001;15:1424–32.
35. Klingmuller U, Lorenz U, Cantley LC, Neel BG, Lodish HF. Specific recruitment of SH-PTP1 to the erythropoietin receptor causes inactivation of JAK2 and termination of proliferative signals. *Cell* 1995;80:729–38.
36. Kunnumakkara AB, Nair AS, Sung B, Pandey MK, Aggarwal BB. Boswellic acid blocks signal transducers and activators of transcription 3 signaling, proliferation, and survival of multiple myeloma via the protein tyrosine phosphatase SHP-1. *Mol Cancer Res* 2009;7:118–28.

## Correction: TMEFF2 Deregulation Contributes to Gastric Carcinogenesis and Indicates Poor Survival Outcome

In this article (Clin Cancer Res 2014;20:4689–704), which was published in the September 1, 2014, issue of *Clinical Cancer Research* (1), the authors provided incorrect versions of Figs. 5A, 5B, 6C, and 6E in the main text and Supplementary Figs. S1 to S6, which were published with the issue. The corrected main text figures are below; the corrected supplementary figures are posted online. In addition, a callout in the final paragraph of the article that reads "Supplementary Fig. S6G" should read "Fig. 6G." The results and conclusions put forth in the article remain unchanged. The authors regret this error.

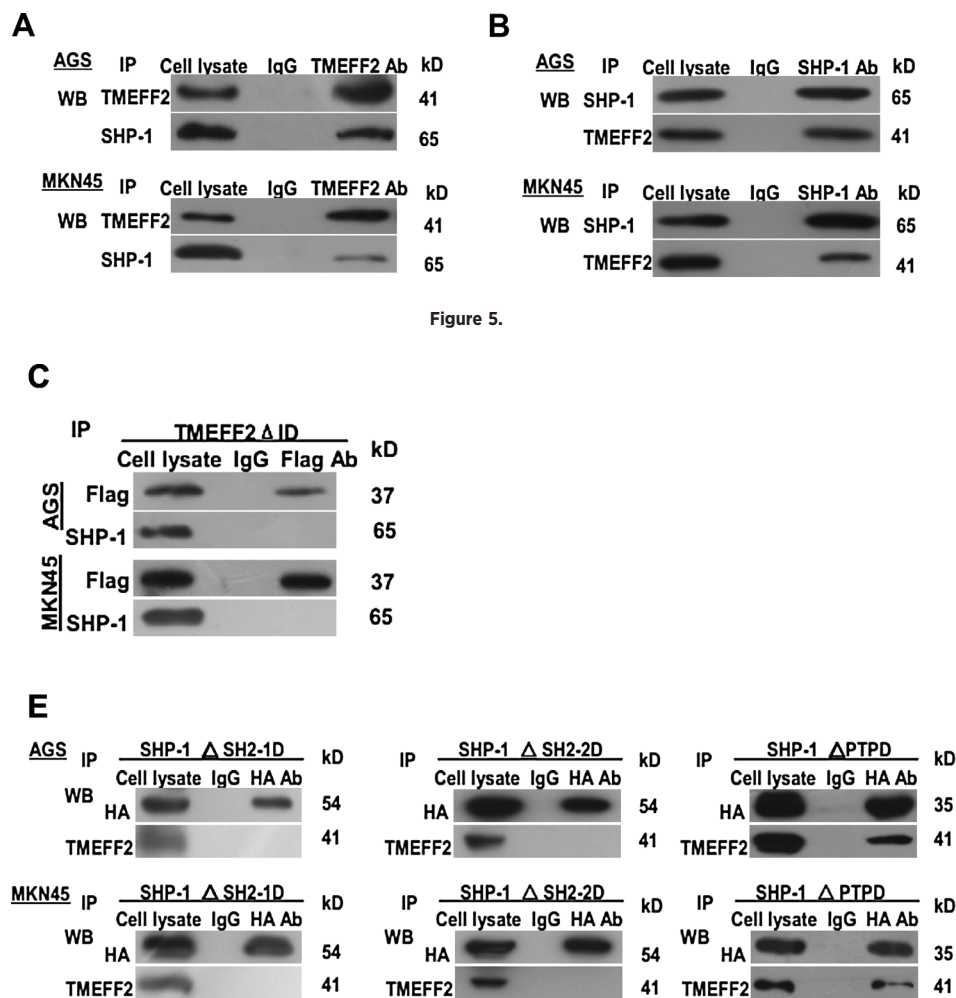


Figure 5.

Figure 6.

### Reference

- Sun T, Du W, Xiong H, Yu Y, Weng Y, Ren L, et al. TMEFF2 deregulation contributes to gastric carcinogenesis and indicates poor survival outcome. Clin Cancer Res 2014;20:4689–704.

Published online August 3, 2015.  
doi: 10.1158/1078-0432.CCR-15-1270  
©2015 American Association for Cancer Research.

# Clinical Cancer Research

## TMEFF2 Deregulation Contributes to Gastric Carcinogenesis and Indicates Poor Survival Outcome

Tiantian Sun, Wan Du, Hua Xiong, et al.

*Clin Cancer Res* 2014;20:4689-4704. Published OnlineFirst July 1, 2014.

**Updated version** Access the most recent version of this article at:  
doi:[10.1158/1078-0432.CCR-14-0315](https://doi.org/10.1158/1078-0432.CCR-14-0315)

**Supplementary Material** Access the most recent supplemental material at:  
<http://clincancerres.aacrjournals.org/content/suppl/2014/07/14/1078-0432.CCR-14-0315.DC1.html>

**Cited articles** This article cites 36 articles, 12 of which you can access for free at:  
<http://clincancerres.aacrjournals.org/content/20/17/4689.full.html#ref-list-1>

**Citing articles** This article has been cited by 1 HighWire-hosted articles. Access the articles at:  
<http://clincancerres.aacrjournals.org/content/20/17/4689.full.html#related-urls>

**E-mail alerts** [Sign up to receive free email-alerts](#) related to this article or journal.

**Reprints and Subscriptions** To order reprints of this article or to subscribe to the journal, contact the AACR Publications Department at [pubs@aacr.org](mailto:pubs@aacr.org).

**Permissions** To request permission to re-use all or part of this article, contact the AACR Publications Department at [permissions@aacr.org](mailto:permissions@aacr.org).